ELSEVIER

Thermochimica Acta 351 (2000) 139–151

thermochimica acta

www.elsevier.com/locate/tca

Studies on (non) energetic compounds Part 20. Preparation and thermolysis of ring-substituted arylammonium bromides

Dr. Gurdip Singh*, Inder Pal Singh Kapoor, Jaspreet Kaur

Chemistry Department, D.D.U. Gorakhpur University, Gorakhpur 273 009, India

Received 16 August 1999; accepted 1 February 2000

Abstract

Ring-substituted arylammonium bromides (RSABr) have been prepared and characterised. Their thermal decomposition has been investigated by TG and DTA techniques. Kinetics of their thermal decomposition was evaluated by both non-isothermal and isothermal data. The proposed thermal decomposition pathways involves simultaneous sublimation, vapourisation and decomposition.

Keywords: Ring-substituted arylammonium bromides; Thermogravimetry; Differential thermal analysis

1. Introduction

Alkyl and arylammonium halides have been reported as phase transfer catalysts [1] and corrosion inhibitors for mild steel [2] in H_2SO_4. The thermal decomposition reaction of ring-substituted arylammonium nitrates [3–5], perchlorates [6–8] and sulfates [9–12] have been explained by postulating dissociation involving proton transfer as the primary step prior to decomposition.

Recently, a number of ring (mono- and di-)-substituted arylammonium chlorides have been prepared and characterised [13–15]. The mechanism of their thermal decomposition has also been proposed. In the light of these findings, thermal decomposition studies on ring-substituted arylammonium bromides (RSABr) have been found to be most interesting.

In the present communication, the thermal decomposition of RSABr has been investigated in detail and the kinetic parameters have been evaluated using isothermal and non-isothermal equations.

2. Experimental

2.1. Materials

Aniline (Qualigens), *m*-toluidine (Johnson Chemical), *p*-toluidine (BDH), *m*-chloroaniline (CDH), *p*-chloroaniline (CDH), *m*-aminobenzoic acid (Merck), *p*-aminobenzoic acid (SISCO), *m*-nitroaniline (Robert Johnson), *p*-nitroaniline (Johnson), *m*-anisidine (Merck), *p*-anisidine (Merck) were purified by usual methods. Hydrobromic acid (CDH), silver nitrate (Qualigens) silica–gel G. for TLC (Qualigens) were used as received.

* Corresponding author. Tel.: +91-0551-200745; fax: +91-0551-340459.
E-mail address: ssdas@ndf.vsnl.net.in (G. Singh)

0040-6031/00/$ – see front matter
PII: S0040-6031(00)00431-7

2.2. Preparation and characterisation of mono-ring-substituted arylammonium bromides (RSABr)

RSABr were prepared by reacting corresponding arylamines with 49% hydrobromic acid in molar ratio 1:1 and reaction can be represented as follows:

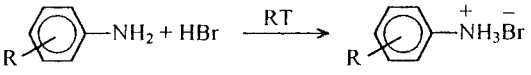

where R=H, *m*-CH_3, *p*-CH_3, *m*-COOH, *p*-COOH, *m*-Cl, *p*-Cl, *m*-NO_2, *p*-NO_2, *m*-OCH_3, *p*-OCH_3.

Instant precipitation were obtained in all the cases at room temperature (25–30°C). The precipitates were washed with petroleum spirit twice to remove unreacted arylamine and then recrystallised from water/alcohol. These salts were dried in incubator at 40±1°C. The purity was checked by TLC and were characterised by elemental, gravimetric and spectral analyses. Their structures, m.p./decomposition temperatures, crystal colour, elemental data, IR and ^{1}H NMR data are summarised in Tables 1 and 2.

2.3. Gravimetric analysis

Two hundred milligrams of each salt was dissolved in 150 ml of water and 0.5 ml conc. HNO_3 was added. Thereafter, $AgNO_3$ was added till precipitation was completed. The precipitates were filtered off in sinterred crucible, washed with ice cold water and dried in hot air oven. Percentage of bromide in each salt is given in Table 1.

2.4. Elemental and spectroscopic analysis

The C, H, N analysis was carried out on Heraeus Carlo–Erba 1108 instrument and percentage of each element is given in Table 1. IR spectroscopy was measured on a Perkin–Elmer 983 DS system using KBr pellets and ^{1}H NMR spectra were recorded using DMSO-D_6 Em 390 (Varian) and data is summarised in Table 2.

2.5. Thermal decomposition of RSABr

2.5.1. Non-isothermal TG

TG studies on RSABr (wt. 30 mg, particle size 200–400 mesh) were undertaken in static air at a heating rate of 5°C min^{-1} using homemade TG apparatus fitted with a temperature indicator cum controller (Model 8087 Century). A bucket type platinum crucible (height=10 mm, diameter=10 mm) was used as sample holder. The fractional decomposition (α) versus temperature plots are shown in Fig. 1. The temperatures corresponding to complete decomposition (T_f) of these salts are listed in Table 3.

2.5.2. Simultaneous TG–DTA

These studies on RSABr (~3.5 mg, 200–400 mesh) were undertaken in N_2 atmosphere using a Mettler Toledo Stare System and weight loss–time plots are given in Fig. 2. The onset, inflection point peak and end temperatures TG (N_2) are also listed in Table 3.

2.5.3. Isothermal TG

Isothermal TG on samples of RSABr (30 mg, 200–400 mesh) was carried out in static air on the same apparatus as described above between 160 and 200°C. The fractional weight loss α versus time (t) plots are reported in Fig. 3.

2.6. Kinetic analysis

2.6.1. Isothermal kinetics

The reaction mechanism was derived by fitting the isothermal TG data to rate expressions [16,17]. The kinetics of thermolysis of RSABr salts was evaluated using nine kinetic models. Only the contracting envelopes equations for n=2 and 3 gave best fits (see Figs. 4 and 5). The calculated kinetic parameters and correlation coefficients (r) are shown in Table 4. This proves that the rate-controlling step in RSABr decomposition is that involving the change in phase boundary.

The nucleation step occurred rapidly over all the surface of a single cube reactant and the interface is established initially; thereafter, in the direction of the centre of the crystal; the reaction rate decreases throughout. If the edges of the initial cube are of length x then after reaction time of t this would be $(x-2k't)$. It follows that [18]

$$\alpha = \frac{x^3 - (x - 2tk')^3}{x^3}$$

where k' is a constant or

$$(1-\alpha)^{1/3} = \frac{1 - 2k't}{x}$$

Table 1
Structure, physical parameters, TLC, elemental and gravimetric analysis of RSABr[a]

Compound No.	Compound	Structure	Crystal colour	Yield (%)	m.p./decomposition temperature (°C)	Spot colour	R_f	p*K*a	Elements[b]			
									C%	H%	N%	Br
a	Anilinium bromide	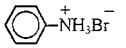	White	56	220	Brown	0.52	4.60	41.92 (41.37)	4.88 (4.59)	7.85 (8.04)	46.201 (45.97)
b	3-Methylanilinium bromide	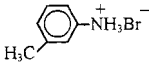	White	68	230	Brown	0.37	4.17	45.99 (44.68)	5.62 (5.31)	7.42 (7.44)	41.02 (42.55)
c	4-Methylanilinium bromide	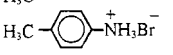	Greyish white	54	225	Yellow	0.51	5.08	44.66 (44.68)	5.58 (5.31)	7.33 (7.44)	43.00 (42.55)
d	3-Carboxylicanilinium bromide	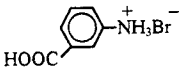	Greyish white	78	230	Brown	0.56	3.07	38.00 (38.53)	3.27 (3.60)	4.19 (6.42)	35.80 (36.6)
e	4-Carboxylicanilinium bromide	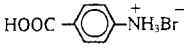	Yellow	80	190	Brown	0.50	2.41	39.02 (38.53)	3.95 (3.60)	6.35 (6.42)	36.00 (36.6)
f	3-Chloroanilinium bromide	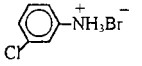	Brown	60	200	Brown	0.63	3.52	39.70 (39.70)	3.50 (3.50)	6.57 (6.71)	16.80 (17.2)
g	4-Chloroanilinium bromide	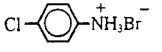	Light brick	70	210	Brown	0.65	3.99	39.8 (39.70)	3.60 (3.50)	6.57 (6.71)	16.70 (17.2)
h	3-Nitroanilinium bromide	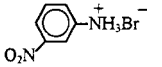	White	68	200	Brown	0.72	2.46	33.18 (33.80)	3.41 (3.17)	12.38 (12.48)	35.80 (36.6)
I	4-Nitroanilinium bromide	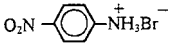	Brown	72	200	Brown	0.60	1.01	33.61 (33.80)	3.51 (3.17)	12.38 (12.48)	35.80 (36.6)
j	3-Methoxyanilinium bromide	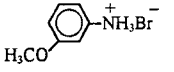	Brick brown	60	180	Brown	0.68	4.20	41.48 (41.10)	5.24 (4.9)	6.74 (6.86)	70.00 (69.21)
k	4-Methoxyanilinium bromide	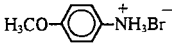	Black	65	200	Brown	0.64	5.29	40.29 (41.10)	5.63 (4.90)	7.51 (6.86)	70.50 (69.2)

[a] Locating reagents, iodine; eluents, hexane:ethyl acetate:alcohol (2:1:1).
[b] Calculated value are in parenthesis.

Table 2
IR and ^{1}H NMR spectra of RSABr

Assignments	Absorption frequencies (cm^{-1}) of RSABr										
	a	b	c	d	e	f	g	h	i	j	k
Primary amine salt (arom.)	3349	3388	3505	3412	3446	3420	3464	3558	3448	3290	3298
ν(N–H)	1593, 1551	1562, 1620	1546, 1717	1621	1546, 1687	1556	1605	1562, 1654	1596, 1625	1668	1606
δ(N–H)	812	895	775	869	901	899	907	915	851	899	815
ν(C–N)	1324	1180	1197	1227	1175	1196	1197	1131	1161	1265	1190
ν(C=C)	1602	1620	1617	1621	1601	1630	1605	1613	1625	1600	1606
m-substituted	–	776	–	801	–	719	–	799	–	777	–
p-substituted	–	–	838	–	780	–	814	–	851	–	815
ν(C–H) in CH_3	–	3004	3023	–	–	–	–	–			
δ(C–H) in CH_3	–	1468	1463	–	–	–	–	–			
ν(C=O, OH–)	–	–	–	1346,2953	1601, 2914	–	–	–			
ν(C–Cl)	–	–	–	–	–	1074	1092	–			
ν(C–NO_2)	–	–	–	–	–	–	–	1466	1445		
ν(C–O–C, O–C, C–H in OCH_3)	–	–	–	–	–	–	–	–		1310, 1445	1318,1436
^{1}H NMR Chemical shift (δ ppm)	7.0–8.3 (m,4H,arom)	7.0–7.8 (m,4H,arom) 2.0–2.4 (s, 3H, CH_3)	7.0–7.7 (m,4H,arom) 2.0–2.4 (s, 3H, CH_3)	7.0–9.0 (m,4H,arom)	7.0–8.5 (m,4H,arom)	7.0–8.3 (m,4H,arom)	7.9–8.4 (m,4H,arom)	7.0–8.3 (m,4H,arom)	5.3–7.0 (m,4H,arom)	6.7–7.5 (m,4H,arom) 4.5–4.7 (s, 3H, OCH_3)	6.6–7.8 (m,4H,arom) 3.7–4.3 (s, 3H, OCH_3)

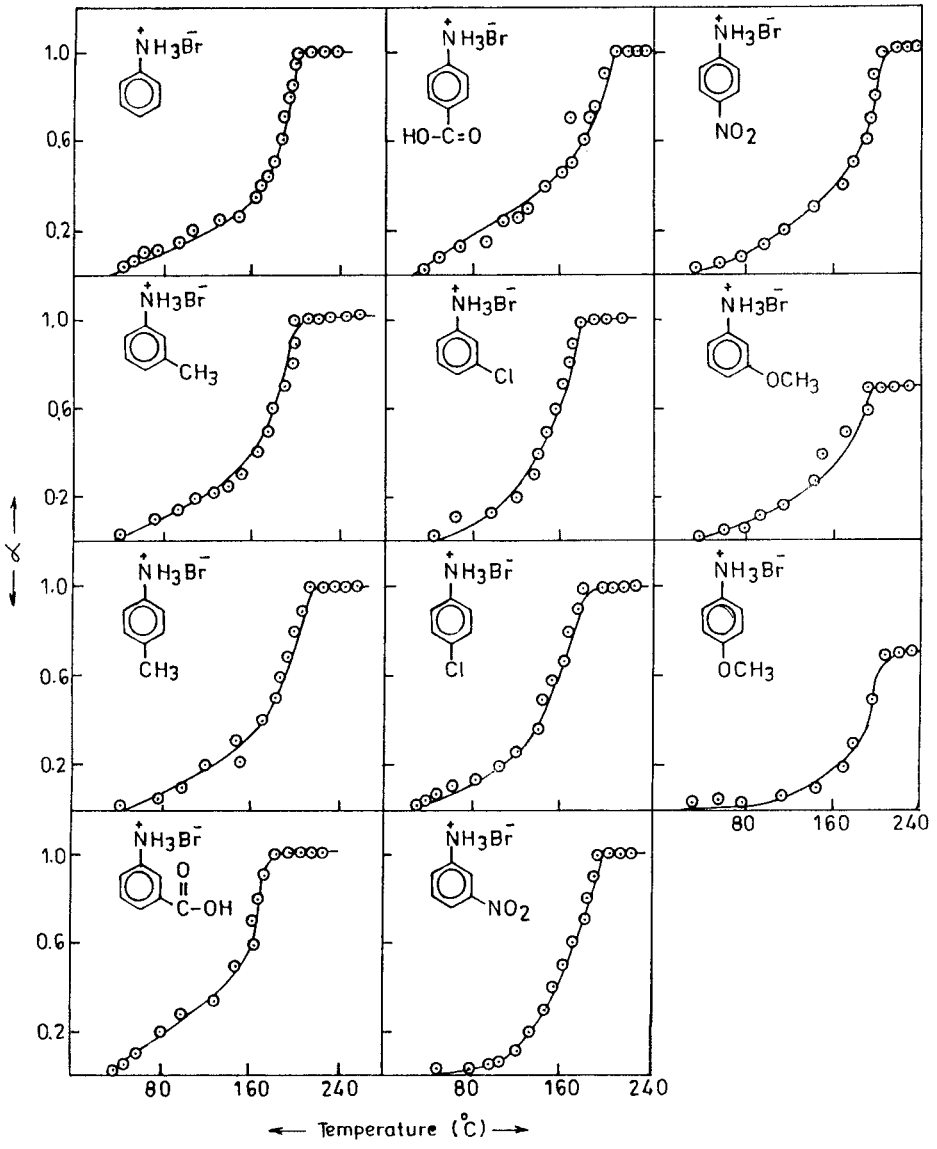

Fig. 1. Non-isothermal TG thermograms of RSABr.

Thus, the contracting reaction envelope becomes

$$1 - (1 - \alpha)^{1/n} = kt \quad (1)$$

where n=2 and 3 and k is rate constant.

The contracting area equation was derived from a model similar to that used for contracting cube equation except that it is assumed that the contact area decreases progressively during reaction.

2.7. Non-isothermal kinetics

Integral methods have been employed to determine the kinetic parameters from non-isothermal TG data. On rearranging and integrating the rate Eq. (2) between the limits α=0 at T_i and α at T, Eq. (3) was obtained.

$$\frac{d\alpha}{dt} = \left(\frac{A}{\phi}\right)\exp\left[\frac{-E_a}{RT}\right]f(\alpha) \quad (2)$$

Table 3
TG and DTA profile data of RSABr

Compound No.	TG (N_2)			DTA (N_2)			Residue (%)	TG (air)
	Onset (°C)	Inflection point (°C)	End (°C)	Onset (°C)	Peak temperature (°C)	Endset (°C)		T_f[a] (°C)
a	218	223	230	184	238	256	1.42	230
b	214	242	246	176	237	259	0.60	230
c	217	245	251	144	245	261	3.59	220
d	252	283	295	193	282	307	10.03	235
e	232	258	266	230	261	274	3.97	200
f	187	212	219	185	215	229	10.67	230
g	202	227	233	202	229	242	1.89	230
h	205	234	239	189	235	249	5.98	230
I	202	247	252	189	208	228	0.20	230
j	205	237	255	243	244	266	0.28	230
k	228	254	282	228	238	267	10.90	230

[a] Temperature at complete decomposition.

$$\int_0^{\alpha} \frac{d\alpha}{(1-\alpha)^n} = \left(\frac{A}{\phi}\right) \int_{T_i}^{T} \exp\left[\frac{-E_a}{RT}\right] dT \qquad (3)$$

The integral of LHS of Eq. (3) is $g(\alpha)$. The right-hand side of Eq. (3) cannot be integrated in a closed form, however, some workers [19] have evaluated the exponential integral by (a) using approximations (b) series expansion and (c) numerical solution method.

Coats–Redfern Eq. (4) was derived by a series expansion method [20,21] and was used to study the kinetics of RSABr

$$\ln\left[\frac{1-(1-\alpha)^{1-n}}{(1-n)T^2}\right] = \ln\left[\frac{AR}{\phi E_a}\left(1-\frac{2RT}{E_a}\right)\right]\frac{E_a}{RT} \qquad (4)$$

where ϕ is the heating rate, E_a the activation energy for the decomposition, α the fractional decomposition at time t and n the order.

Table 4
Arrhenius parameters and correlation coefficient for isothermal decomposition of RSABr

	Contracting area (n=2)							Contracting cube (n=3)						
	Rate constant ($k\times10^{-3}$) min^{-1} at temperature (°K)					r	E (kJ mol^{-1})	Rate constant ($k\times10^{-3}$) min^{-1} at temperature (°K)					r	E_a (kJ mol^{-1})
	433	443	453	463	473			433	443	453	463	473		
a	6.03	10.0	20.0	50.0	125.0	0.9900	114.9	4.0	7.0	14.0	16.0	60.0	0.9531	95.7
b	8.00	16.0	33.0	56.0	100.0	0.9992	114.8	5.2	11.0	20.0	30.0	83.0	0.9748	95.7
c	8.00	12.0	22.0	40.0	60.0	0.9981	76.7	6.0	10.0	25.0	30.0	83.0	0.9846	86.1
d	10.00	18.0	25.0	50.0	100.0	0.9370	184.8	9.0	30.0	60.0	66.0	75.0	0.9130	95.7
e	6.10	12.5	13.5	29.0	50.0	0.9733	185.2	4.0	10.0	15.0	25.0	30.0	0.9764	76.5
f	16.0	12.0	28.0	50.0	70.0	0.9893	99.7	9.0	16.0	30.0	60.0	150.0	0.9890	99.7
g	4.2	10.0	24.0	28.0	40.0	0.9762	94.7	3.3	6.5	10.0	18.0	28.9	0.9966	95.7
h	6.0	90.0	20.0	40.0	120.0	0.9860	153.2	4.0	8.0	15.0	27.0	66.0	0.9978	133.7
I	6.0	7.5	11.7	20.0	30.0	0.9876	114.9	4.0	8.0	11.0	25.0	50.0	0.9876	76.5
j	10.0	30.0	7.5	15.4	200.0	0.9834	113.9	25.0	28.0	6.2	13.6	25.0	0.9634	133.9
k	25.0	37.0	55.0	78.0	140.0	0.9909	38.2	20.0	49.0	70.0	92.0	100.0	0.9050	57.4

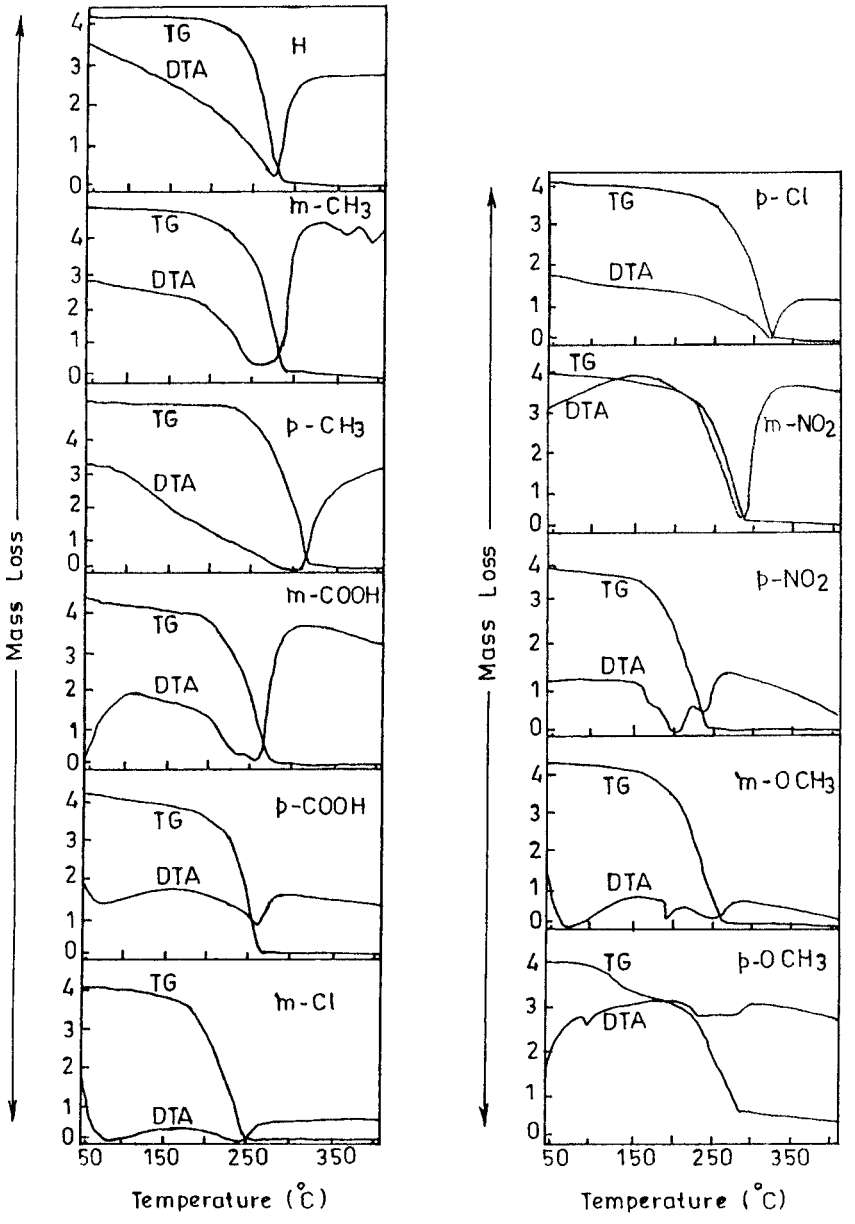

Fig. 2. Simultaneous TG–DTA thermograms of RSABr.

Using the numerical solution method, the rate equation was integrated as:

$$g(\alpha) = \frac{AE_a}{\phi R}\left[\frac{-e^x}{x} + \int_{\infty}^{x}\frac{e^x}{x}dx\right] = \frac{AE_a}{\phi R}p(x) \quad (5)$$

where $x=E_a/RT$.

MacCallum and Tanner (MCT) [22] have derived a Eq. (6) to calculate the kinetic parameters from different curve fittings with the tabulated values of $p(x)$.

$$\ln g(\alpha) = \ln\left[\frac{AE_a}{\phi R}\right] - 0.485E_a^{0.435} - \frac{[0.449 + 0.217E_a]}{T} \times 10^3 \quad (6)$$

where $g(\alpha)=1-(1-\alpha)^{1-n}/1-n$.

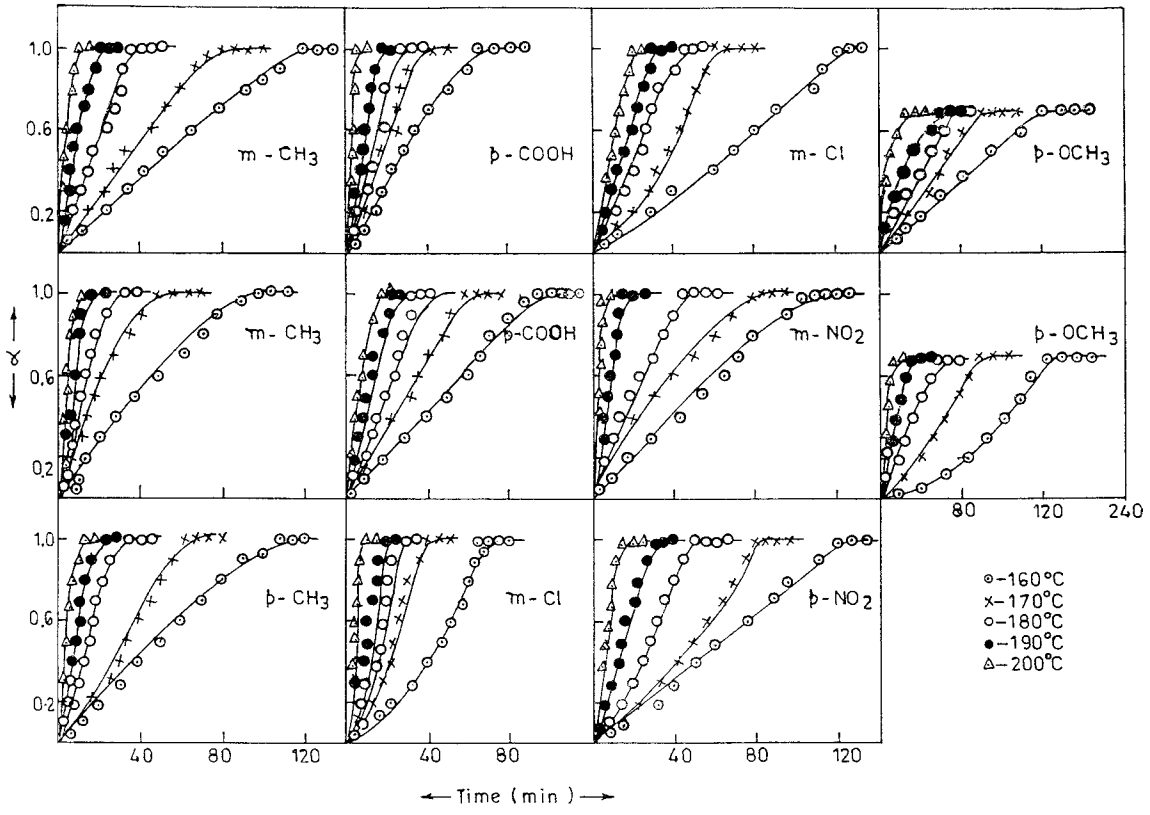

Fig. 3. Isothermal TG thermograms of RSABr.

Madhusudanan et al. [23] have proposed a new simple approximation Eq. (7) for solving the $p(x)$ function.

$$p(x) = \frac{e^{-x}}{x^2}\left[\frac{(x+1)}{(x+3)}\right] \quad (7)$$

It has been shown that $\ln p(x)$ is a linear function of x and the slope and intercept of $\ln p(x)$ versus x curves are linear function of $1/x$ and $\ln(x)$, respectively. On combining these, the Eq. (8) was obtained.

$$\ln p(x) = a + bx + c \ln x \quad (8)$$

On substituting the numerical values of a, b and c, values of $p(x)$ were determined which was substituted in Eq. (5) and rearranged to get Madhusudanan Krishnan–Ninnan (MKN) Eq. (9).

$$\ln\left[\frac{1-(1-\alpha)^{1-n}}{(1-n)T^{1.9215}}\right] = \ln\frac{AE_a}{\phi R} + 3.7721 - 1.9215 \ln E_a \frac{0.12039E_a}{T} \quad (9)$$

The values of activation energies and correlation coefficients (r) obtained from CR, MCT and MKN equations are represented in Table 5.

3. Discussion

Elemental, gravimetric, and spectral data reported in Tables 1 and 2 clearly confirm the formation of RSABr. TG both in N_2 and air (see Figs. 1 and 2) show that all the salts lost ≈100% of their mass in static air and only a small amount of residue was obtained in the case of TG in N_2 (Table 3). Lower T_f values were also observed compared to the end temperatures which may be due to the oxidising behaviour of the surrounding atmosphere. The decomposition pathways reported in Scheme 1 suggest that the thermal decomposition of RSABr salts involves simultaneous sublimation/vapourisation and decomposition processes. It seems that all salts in

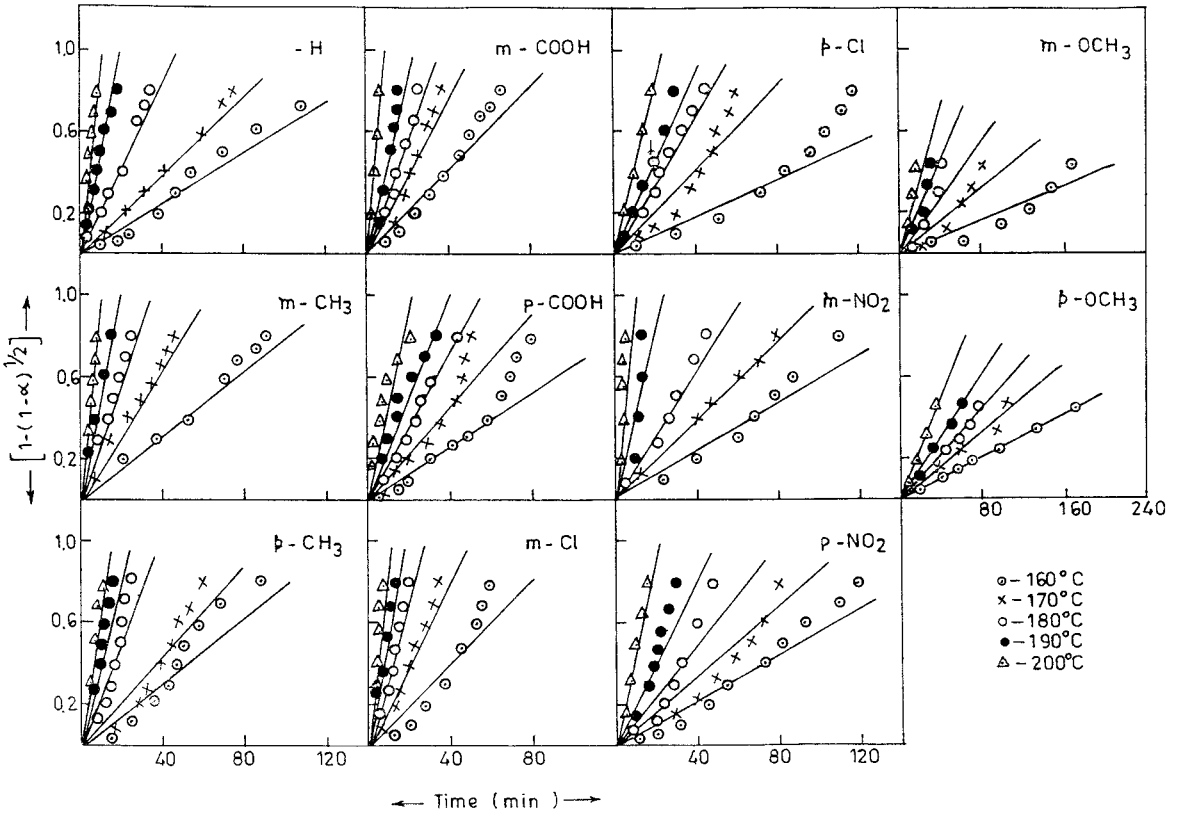

Fig. 4. Kinetic analysis of RSABr by contracting area (n=2) equation.

the solid phase undergo sublimation to form aerosol [24–26]. Moreover, the thermal stability of RSABr may depend upon the tendency of arylammonium ion to release a proton to the bromide ion. The tendency of bromide ion to accept a proton depends on its basicity at higher temperatures [27,28]. Proton transfer [3–15] via an activated complex is assumed as a primary rate-determining step which leads to the formation of the corresponding arylamine and HBr both in the condensed as well as gaseous phase (Scheme 1). Finally, decomposition takes place by the interaction between amine and HBr in the condensed or gaseous phases to form products and residual carbon.

The data reported in Table 3 clearly shows that for the 4-carboxylcanitinium bromide has the highest inflection point and peak temperature while the 3-chloronalinium has the lowest values. The DTA (Fig. 2) of these salts show that all the salts decompose endothermally.

The activation energies reported in Table 4 are in the range 57–189 kJ mol^{-1} which may be due to the simultaneous processes (sublimation/vapourisation/decomposition). The inflection point (TG curve) and E_a show a linear relationship with the (pKa) of the corresponding amine [29] (Fig. 6). This clearly confirms the dependence of thermal stability of these bromide salts on the alkalinity of the arylamines.

Hammett equation [30–32] (Eq. (10)) was also fitted to the thermolysis of RSABr, i.e.

$$\log\left(\frac{k}{k_0}\right) = \rho\sigma \tag{10}$$

where log (k/k_0) is the relative rate ρ is the reaction constant and σ the Hammett substituent constant. Log (k/k_0) varied linearly with σ (see (Table 6 and

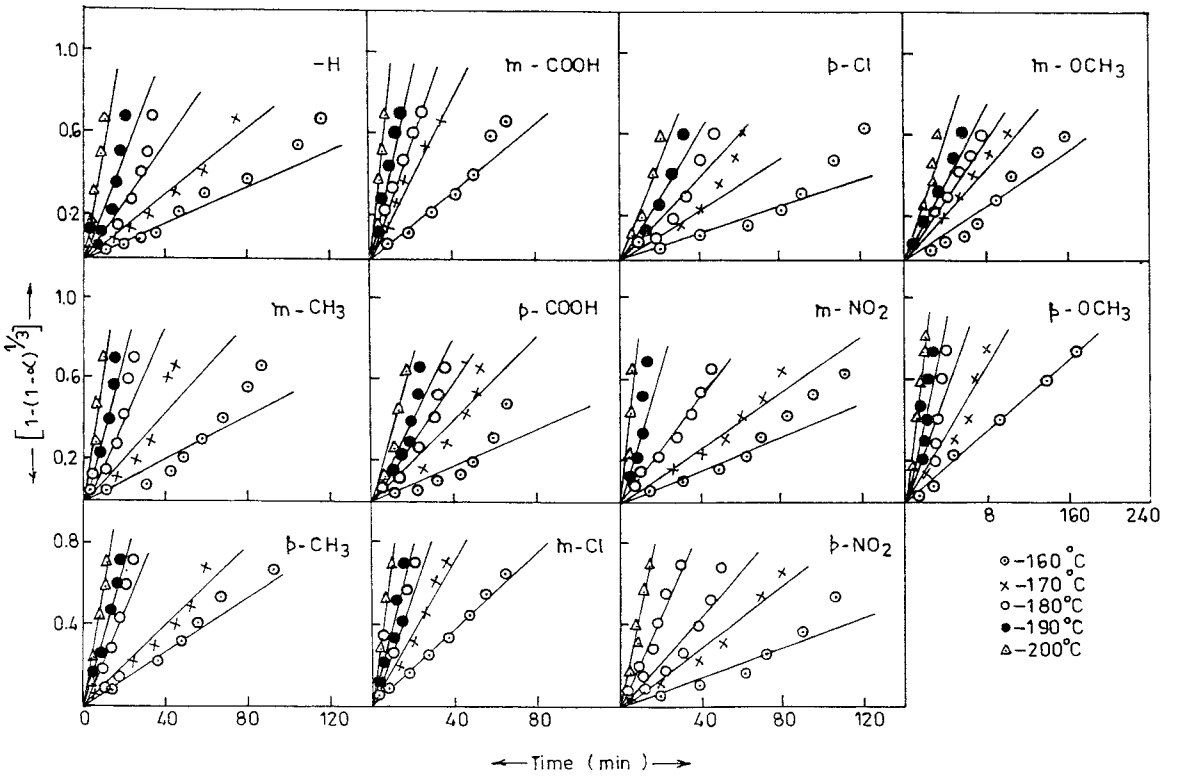

Fig. 5. Kinetic analysis of RSABr by contracting cube (n=3) equation.

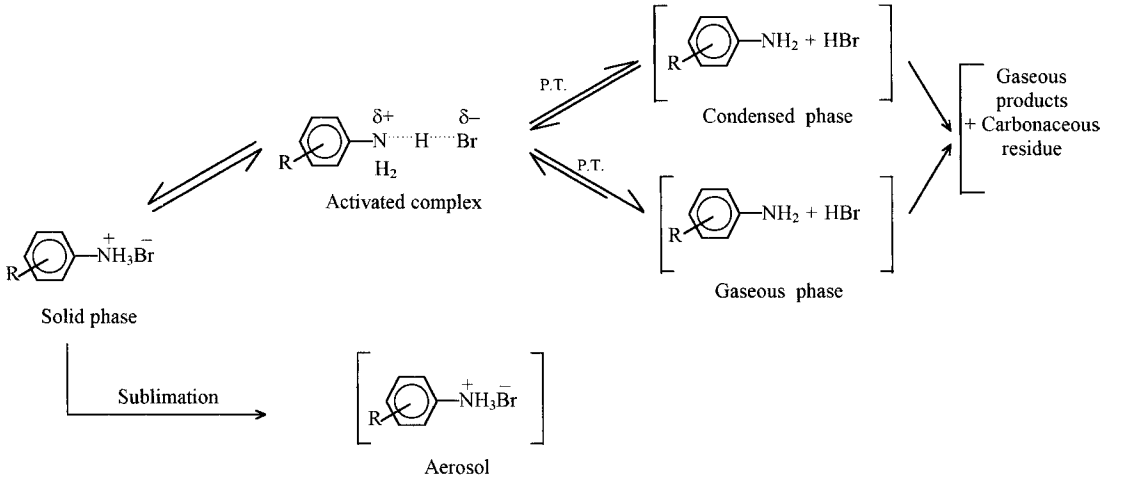

Scheme 1. Thermal decomposition pathways of RSABr.

Table 5
Correlation coefficient (r), activation energy (E_a) for non-isothermal TG data of RSABr

Compound No.	n=0		n=1		n=1/2		n=2/3	
	r	E_a (kJ mol^{-1})	r	E_a (kJ mol^{-1})	r	E_a (kJ mol^{-1})	r	E_a (kJ mol^{-1})
Madhusudanan Krishnan–Ninnan								
a	0.9779	199.8	0.9682	198.8	0.9626	154.6	0.9321	173.4
b	0.9632	263.7	0.9827	40.9	0.9921	93.2	0.0000	61.9
c	0.9743	217.3	0.9631	61.8	0.9708	111.6	0.9727	295.5
d	0.9058	91.1	0.9216	59.7	0.9629	72.3	0.9114	163.8
e	0.9953	127.9	0.9806	62.7	0.9968	72.7	0.9953	71.0
f	0.9181	131.6	0.9467	53.0	0.9348	106.5	0.9181	159.6
g	0.9557	190.1	0.9701	175.5	0.9695	114.1	0.9557	53.5
h	0.9583	159.6	0.9677	34.6	0.9705	95.7	0.9582	53.1
I	0.8119	132.9	0.8753	199.8	0.9083	137.5	0.9682	239.5
j	1.0000	114.1	0.8892	47.6	0.9512	95.7	0.8680	47.6
k	0.8688	91.1	0.8837	39.0	0.9703	72.3	1.0000	43.0
Coats–Red fern								
a	0.9777	324.7	0.9985	46.8	0.9602	47.6	0.8209	152.2
b	0.9396	54.7	0.0	163.0	0.9924	359.4	0.9404	10.9
c	0.9726	207.7	0.9180	326.0	0.9599	288.4	0.8981	52.2
d	0.8550	112.8	0.9218	96.1	0.9068	142.1	0.8433	33.0
e	0.9236	58.9	0.9863	131.6	0.9852	109.9	0.9514	22.9
f	0.9562	119.1	0.9505	144.6	0.9396	58.9	0.8885	23.0
g	0.9493	99.9	0.9718	125.4	0.9732	142.9	0.9199	19.2
h	0.9348	253.7	0.9645	129.5	0.9667	142.8	0.9202	21.3
I	0.8958	89.8	0.9007	129.6	0.8608	42.4	0.8410	17.5
j	0.8505	91.9	0.9482	122.8	0.9010	122.4	0.9291	20.0
k	0.8429	95.4	0.9304	114.1	0.8802	213.1	0.9611	17.5
Mac Callum Tanner								
a	0.9926	82.7	0.9750	81.0	0.9501	81.0	0.8375	82.7
b	0.9948	84.8	0.9939	66.8	0.9550	66.8	0.9323	84.4
c	0.9960	84.4	0.9787	84.4	0.9450	84.8	0.8886	84.8
d	0.9814	86.1	0.9644	66.8	0.9930	84.8	0.8889	84.8
e	0.9902	86.1	0.9934	66.8	0.9980	85.6	0.8607	84.8
f	0.9913	84.4	0.9709	66.8	0.0000	84.4	0.8518	84.8
g	0.9972	84.5	0.9887	84.8	1.0000	86.1	0.8990	85.2
h	0.9948	86.1	0.9823	84.8	0.8816	86.1	0.8944	85.2
I	0.9603	84.8	0.9282	84.9	0.8798	84.8	0.8010	85.2
j	0.9804	86.1	0.9970	66.8	0.9274	84.8	0.8581	84.4
k	0.9578	66.8	0.9760	84.9	0.9657	86.1	0.8861	85.3

Table 6
Relative rates for thermal decomposition of RSABr and $\sigma\pm$ for corresponding amines

Relative rates (°C)	RSABr										
	a	b	c	d	e	f	g	h	i	j	k
log (k/k_0)170 (CA)[a]	0.0	0.2041	0.0790	−0.2552	0.0969	0.0791	0.1172	0.0457	−0.1249	−0.4771	−0.5682
log (k/k_0)170 (CC)[b]	0.0	0.1962	0.1549	0.6320	0.1549	0.3549	−0.0320	0.0579	0.5799	0.6020	0.8450
($\sigma\pm$)	0.0	0.0700	0.1700	0.3600	0.4100	0.3700	0.2300	0.7100	0.7800	−0.1200	−0.6600

[a] Contracting area (n=2).
[b] Contracting cube (n=3) equations.

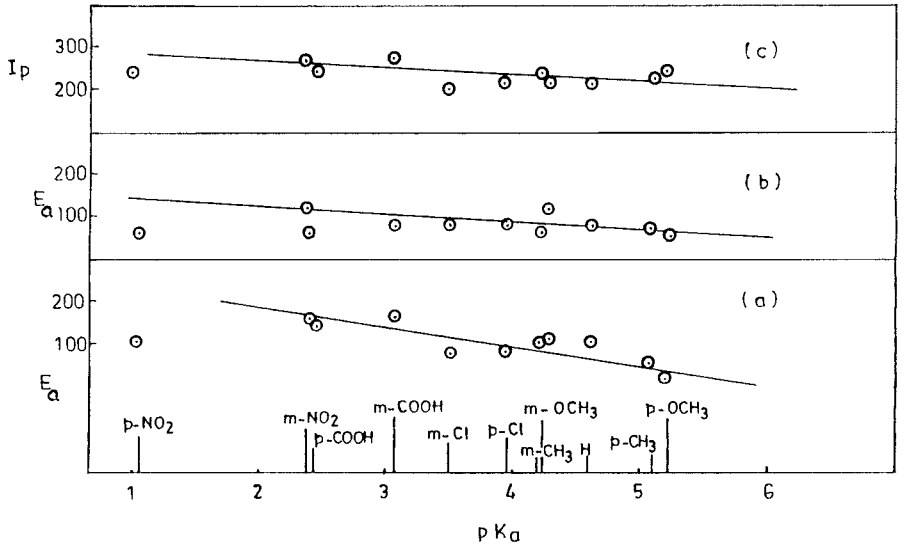

Fig. 6. Plots of p*K*a vs. (a) activation energy (E_a) for contracting area (n=2) equation; (b) activation energy (E_a) for contracting cube (n=3) equation; (c) inflection point from TG thermogram in N_2 atmosphere.

Fig. 7), and it can be inferred that the same mechanism is operating throughout the series. The reaction constant (ρ) was found to be +0.40. A positive value for ρ indicates [33] that the thermal decomposition of RSABr is facilitated by electron-accepting substituents. Some of the substituents deviated markedly for the linear behaviour and this may be due to large resonance-inductive effects of *m*- and *p*-substituents.

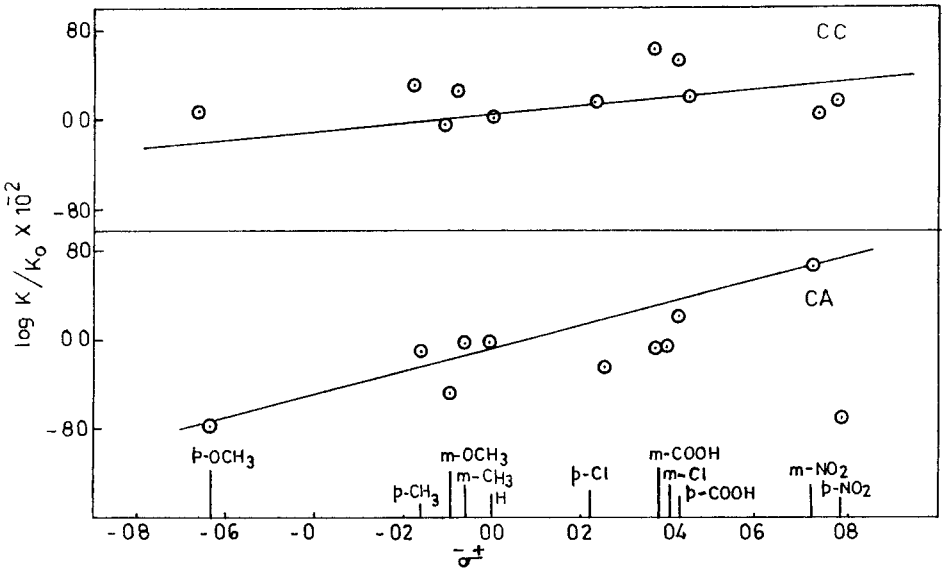

Fig. 7. Plots of log (k/k_0) vs. Hammett substituent constant ($\sigma\pm$) for RSABr.

Acknowledgements

We are grateful to the Head of the Chemistry Department for providing laboratory facilites, and the financial assistances of DST and UGC are also acknowledged. Thanks are also due to RSIS, Nagpur for TG–DTA and CDRI, Lucknow for elemental and spectroscopic analyses.

References

[1] U.T. Bhalerao, S.N. Mathur, S.N. Rao, Synthetic Comm. 22 (1992) 1645.
[2] B.V. Savithri, S.M. Mayannan, Indian J. Chem. Tech. 3 (1996) 256.
[3] G. Singh, I.P.S. Kapoor, S.M. Mannan, Thermochim. Acta. 262 (1995) 117.
[4] G. Singh, I.P.S. Kapoor, S.M. Mannan, J.P. Agrawal, Combust. Flame 97 (1994) 355.
[5] G. Singh, I.P.S. Kapoor, Combust. Flame 92 (1993) 283.
[6] G. Singh, I.P.S. Kapoor, S.M. Mannan, J. Therm. Anal. 46 (1996) 1751.
[7] G. Singh, I.P.S. Kapoor, S.M. Mannan, J. Energ. Mat. 13 (1992) 141.
[8] G. Singh, I.P.S. Kapoor, S.M. Mannan, J. Energ. Mat. 13 (1995) 141.
[9] G. Singh, I.P.S. Kapoor, M. Jain, Thermochim. Acta 292 (1997) 135.
[10] G. Singh, I.P.S. Kapoor, J. Chem. Soc. Perkin Trans II (1989) 2155.
[11] G. Singh, I.P.S. Kapoor, M. Jain, J. Chem. Soc. Perkin Trans II (1993) 1521.
[12] G. Singh, I.P.S. Kapoor, J. Kaur, Thermochimica Acta, 1999 (in press).
[13] G. Singh, I.P.S. Kapoor, J. Kaur, Indian. J. Chem. 38B (1999) 56.
[14] G. Singh, I.P.S. Kapoor, J. Kaur, Thermochim. Acta, 338 (1995) 45.
[15] G. Singh, I.P.S. Kapoor, J. Kaur, Indian. J. Chem. Tech., 1999 (communicated).
[16] V. Satava, Thermochim. Acta 2 (1971) 423.
[17] J.H. Sharp, G.W. Brindley, B.N.N. Achar, J. Am. Ceram. Soc. 49 (1966) 379.
[18] A.K. Galwey, Chemistry of Solids, Chapman and Hall, London, 1967, 179 pp.
[19] K.N. Ninnan, J. Therm. Anal. 35 (1989) 1267.
[20] A.W. Coats, J.P. Redfern, Nature (London) 20 (1964) 88.
[21] A.W. Coats, J.P. Redfern, Polym. Lett. 3 (1965) 917.
[22] J.R. MacCallum, J. Tanner, Eur. Polym. J. 6 (1970) 1033.
[23] P.M. Madhusudanan, K. Krishnan, K.N. Ninnan, Thermochim. Acta 97 (1987) 189.
[24] W.A. Rosser, S.H. Inami, H. Wise, J. Phys. Chem. 67 (1963) 1753.
[25] T.P. Russel, T.B. Brill, Combust. Flame 76 (1989) 393.
[26] D.G. Patil, S.R. Jain, T.B. Brill, Propell. Explosives Pyrotechn. 17 (1962) 99.
[27] L. Erdey, S. Gal, Talanta 10 (1963) 23.
[28] L. Erdey, S. Gal, G. Liptay, Talanta 11 (1964) 913.
[29] J.C. Dean, Lange's Handbook of Chemistry, 13th Edition, McGraw-Hill, New York, 1985.
[30] C.D. Johnson, The Hammet Equation, Cambridge University Press, Cambridge, 1973.
[31] L.P. Hammet, Physical Organic Chemistry, McGraw-Hill, New York, 1940, 184 pp.
[32] H.H. Jaffe, Chem. Rev. 53 (1953) 191.
[33] R.A.Y. Jones, Physical and Mechanistic Organic Chemistry, 2nd Edition, Cambridge University Press, New York, 1989, 42 pp.